

Psilocybin reduces functional connectivity and the encoding of spatial information by neurons in mouse retrosplenial cortex

Victorita Ivan¹, David Tomas-Cuesta¹, Ingrid Esteves¹, Artur Luczak¹, Majid Mohajerani¹, Bruce McNaughton², and Aaron Gruber¹

¹University of Lethbridge

²Lethbridge University

April 22, 2024

Abstract

Psychedelic drugs have profound effects on perception, cognition, and mood. How psychedelics affect neural signaling to produce these effects remains poorly understood. We investigated the effect of the classic psychedelic psilocybin on neural activity patterns and spatial encoding in the retrosplenial cortex of head-fixed mice navigating on a treadmill. The place specificity of neurons to distinct locations along the belt was reduced by psilocybin. Moreover, the stability of place-related activity across trials decreased. Psilocybin also reduced the functional connectivity among simultaneously recorded neurons. The 5-HT_{2A}R (serotonin 2A receptor) antagonist ketanserin blocked the majority of these effects. These data are consistent with proposals that psychedelics increase the entropy of neural signaling, and provide a potential neural mechanism contributing to disorientation frequently reported by humans after taking psychedelics.

**Psilocybin reduces functional connectivity and the encoding of spatial information by
neurons in mouse retrosplenial cortex**

Victorita E. Ivan^{1*}, David P. Tomàs-Cuesta^{1*}, Ingrid M. Esteves¹, Artur Luczak¹, Majid¹
Mohajerani^{1,2}, Bruce L. McNaughton^{1,3}, Aaron J. Gruber¹✉

¹Canadian Center for Behavioural Neuroscience, Department of Neuroscience, University of
Lethbridge, Lethbridge, Alberta, Canada

²Douglas Research Centre, Department of Psychiatry, McGill University

³Center for the Neurobiology of Learning and Memory, University of California Irvine, Irvine,
California, USA

*The authors contributed equally.

✉ Aaron J. Gruber

Email: aaron.gruber@uleth.ca

Keywords: retrosplenial cortex, psychedelics, ketanserin, mutual information, serotonin

1 **Abstract**

2 Psychedelic drugs have profound effects on perception, cognition, and mood. How psychedelics
3 affect neural signaling to produce these effects remains poorly understood. We investigated the
4 effect of the classic psychedelic psilocybin on neural activity patterns and spatial encoding in the
5 retrosplenial cortex of head-fixed mice navigating on a treadmill. The place specificity of neurons
6 to distinct locations along the belt was reduced by psilocybin. Moreover, the stability of place-
7 related activity across trials decreased. Psilocybin also reduced the functional connectivity among
8 simultaneously recorded neurons. The 5-HT_{2A}R (serotonin 2A receptor) antagonist ketanserin
9 blocked the majority of these effects. These data are consistent with proposals that psychedelics
10 increase the entropy of neural signaling, and provide a potential neural mechanism contributing to
11 disorientation frequently reported by humans after taking psychedelics.

12

13

14

15

16

17

18

19

20

21 **Introduction**

22 Psychedelic drugs have profound acute effects on perception, cognition, and mood. Molecules
23 affecting a variety of neurotransmitter receptor types have psychedelic properties. The serotonin,
24 or hydroxytryptophan (5-HT), 2A receptor has been identified as the primary mediator of the
25 psychedelic effects of classic psychedelics, such as psilocybin (Vollenweider et al., 1998;
26 Quednow et al., 2012). 5-HT can modulate neural activity in the brain's neocortex through
27 presynaptic and postsynaptic neuromodulatory effects on cortical neurons (Andrade, 2011), which
28 express a variety of 5-HT receptor types. Several primary effects of psilocybin are blocked by the
29 5-HT_{2A} antagonist ketanserin (Kometer et al., 2012; Torrado Pacheco et al., 2023). Ketanserin,
30 however, does not block all of its effects (Carter et al., 2005; Hesselgrave et al., 2021). Therefore,
31 non-5-HT_{2A} receptors likely contribute to the effects of psilocybin on mentation.

32 The effects of psilocybin on neural encoding and brain dynamics have largely been studied using
33 non-invasive imaging in humans (Carhart-Harris et al., 2012; Carhart-Harris et al., 2017b; Daws
34 et al., 2022). This work suggests that the coordination of activity among brain regions becomes
35 less structured (Muthukumaraswamy et al., 2013; Varley et al., 2020). It remains to be determined
36 if this also occurs at the level of neurons, and if this is due more to corruption of the inputs to
37 cortical networks involved in perception, or more due to corruption of the dynamics within these
38 networks. The few existing studies of cellular-level effects in behaving animals report discrepant
39 effects. A recent study of visual cortex showed little effect of a classic psychedelic (2,5-dimethoxy-
40 4-iodoamphetamine; DOI) on responses to visual inputs in mouse primary visual cortex (Michaiel
41 et al., 2019). On the other hand, we reported that the non-classic psychedelic ibogaine significantly
42 degrades the encoding of spatial information in a cortical region called the retrosplenial cortex
43 (RSC) (Ivan et al., 2023). The discrepancy between these studies may involve differences in brain

44 region and/or the pharmacology of the psychedelic used. Here, we test if the classic psychedelic
45 psilocybin degrades spatial information similarly to ibogaine, and if this depends on 5-HT_{2A}
46 receptors.

47 The RSC encodes the spatial state of animals within an environment and supports navigation in
48 freely moving animals (Keene and Bucci, 2009; Alexander and Nitz, 2015). Some RSC neurons
49 activate when an animal traverses specific regions of an environment, similar to ‘place cells’ in
50 the hippocampus (O'Keefe and Nadel, 1978). RSC neurons generate similar place cells in head-
51 fixed animals navigating virtual environments (Mao et al., 2017; Esteves et al., 2021). The RSC is
52 a key node in a network linking the hippocampus (HPC) with the medial prefrontal cortex (mPFC)
53 (Wyass and Van Groen, 1992; Fisk and Wyss, 1999; Shibata et al., 2004). This network is involved
54 in generating representations of environments via cognitive maps (O'Keefe and Nadel, 1978; Iaria
55 et al., 2007), and navigation decisions to achieve goals. 5-HT appears to affect this processing.
56 Psilocin, psilocybin's active metabolite, causes a decrease in the BOLD signal relative to baseline
57 in the cingulate and retrosplenial cortical regions of rats (Spain et al., 2015). Conversely, resting-
58 state fMRI in anesthetized mice found an increase in functional connectivity (FC) between these
59 two regions and other structures expressing the 5-HT_{2A} receptors, such as the ventral striatum
60 (Grandjean et al., 2021). RSC interactions with other structures thus appears to be modulated by
61 psychedelics. The spatial information encoded in this region provides a means to assess how these
62 psychedelics affect neural information processing at the cellular level. Here, we quantify how
63 psilocybin, with or without blockage of 5-HT_{2A} receptors, affect spatial representation and neural
64 dynamics of large ensembles of neurons in RSC as head-fixed mice navigate a virtual environment.

65

66

67 **Methods**

68 *Animals*

69 Adult (4-9 month old) Thy1-GCaMP6m mice (n=10; 2F/8M), weighing 19-28 g, were housed in
70 standard rodent cages, and maintained at 24 °C under a 12 h light/dark cycle. Mice had free access
71 to food and water before training. All experiments were performed during the light cycle (between
72 7:30 AM and 7:30 PM). Procedures were in accordance with the guidelines established by the
73 Canadian Council on Animal Care, and with protocols approved by the Animal Welfare
74 Committee of the University of Lethbridge.

75 *Surgery*

76 Before surgery, animals received buprenorphine (0.05 mg/kg SC) and dexamethasone (0.2 mg/kg
77 IM). They were then anesthetized with isoflurane (1-1.5%) and head fixed in a stereotaxic frame
78 with body temperature maintained at 37.0 ± 0.5 °C with a heating pad. Mice received a 5 mm
79 bilateral craniotomy (AP: +1 to -4; ML: -2.5 to +2.5), which was then covered with three layers of
80 coverslips affixed with optical adhesive (NOA71, Norland). The coverslip was attached to the
81 skull using Vetbond, and a titanium head plate was fixed to the skull using metabond. Post-surgical
82 care included careful weight monitoring and subcutaneous injections of meloxicam (Metacam 1
83 mg/kg) and enrofloxacin (Baytril, 10 mg/kg) for three days after implant.

84 *Drugs*

85 Psilocybin was obtained from Toronto Research Chemicals, Canada, in powder form and diluted
86 in sterile water in order to achieve a dose of 1.5 or 15 mg/kg in a 0.1 ml volume for each mouse.

87 Ketanserin tartrate salt was obtained from Sigma-Aldrich Canada, in powder form, and dissolved
88 in 20% DMSO, and the stock solutions were stored at -20°C . The stock solutions were prepared
89 on the day of injection when possible and diluted in saline to achieve a dose of 1 or 5 mg/kg. The
90 control animals received 0.1 ml 0.9% saline solution. All injections were intraperitoneal.

91 *Experimental procedure for behaviour*

92 Head-fixed mice were trained to run on a treadmill using a positive reinforcement paradigm. They
93 received a drop of 10% sucrose solution on every trial, consisting of one lap of the treadmill belt.
94 Animals were water restricted during the training and testing. They had ad libitum access to water
95 for up to 30 minutes per day, and their body weight was carefully monitored throughout the
96 experiment to ensure the weight loss did not exceed 15% of their baseline value. The treadmill belt
97 consisted of a Velcro strip that was 150 cm long and 4 cm wide. Three tactile cues were placed in
98 different locations on the belt. Additionally, we used one auditory cue (1kHz) and one blue light
99 LED cue that each activated at a specific and constant belt position. An optical encoder attached
100 to the wheel shaft was used to monitor belt movement. A microcontroller was used to monitor the
101 encoder, licking sensor, and the reward delivery. Training continued in daily sessions until mice
102 performed at least 20 trials in 20 minutes. Mice were trained on one belt and then transferred to a
103 new belt for the imaging sessions.

104 Neural activity was imaged in daily sessions of the task for 15-20 minutes. For drug days, we
105 recorded first a baseline activity (+/- saline/ketanserin) for 10 mins in every session, then mice (n
106 = 7) were given an injection of psilocybin or saline and recorded again for 10 minutes. Recordings
107 were performed starting at 10 minutes after each injection. Each animal was imaged for one session
108 before any injections, for two days of saline injections, and then received 4 days of psilocybin

109 every other day, with or without the ketanserin pretreatment. The control group (n = 3) received
110 only saline in the same schedule as the treatment group.

111 *Two-Photon Imaging*

112 Neural activity was imaged using a 2-photon microscope (Bergamo II multiphoton microscopy,
113 Thorlabs) through a 16x water-immersion objective lens (NA=0.8, Nikon). Excitation was with a
114 Ti:sapphire pulsed laser (Coherent) tuned to a wavelength of 920 nm, ~80mW power, and
115 controlled by a galvo-resonant X-Y scanner. Images were acquired at depths between 135 μm –
116 160 μm (layer II/III), from a field of view of 835 x 835 μm . Images were digitized at a sampling
117 rate of 19 Hz, and at a resolution of 800 x 800 pixels. Imaging data from all animals were acquired
118 from one hemisphere of either the left or right RSC (AP: -1 to -3 mm; ML: 0 to +/- 1 mm).

119 *Pre-processing*

120 Automatic image pre-processing was performed using the Suite-2P algorithm (Pachitariu et al.,
121 2017), as previously described (Mao et al., 2017; Mao et al., 2018). The regions of interest (ROIs)
122 detected were inspected manually and labelled as cells or non-cells by experienced users. For each
123 ROI, the $\Delta F/F$ time courses were deconvolved using constrained non-negative matrix factorization
124 (Pnevmatikakis et al., 2016), and all subsequent analyses were conducted using the deconvolved
125 time-courses. For injection days, the imaging sequences of both pre- and post-injection intervals
126 were combined during pre-processing so as to acquire the activity of the same set of cells (ROIs)
127 before and after injections.

128 *Computing spatial encoding*

129 In order to identify spatially tuned neurons, we computed the adjusted mutual information (MI)
130 (Vinh et al., 2010) between the firing rate of each neuron and the position of the mouse in the belt.
131 We first divided the belt into 50 bins (3 cm each). For each bin and trial, we summed the neuron's
132 activity and binned it into 4 levels, giving us the joint bin-activity discrete distribution, which we
133 use to compute the mutual information. The MI used here is an adjustment of mutual information
134 which accounts for the number of trials, which differs number among session, and thus is
135 appropriate to compare cells from different sessions on the same scale. The MI is upperlimited by
136 1 and takes an expected value of 0 when the firing and position are independent. Negative values
137 signify that the MI for that cell is lower than the MI one would expect solely due chance.

138 *Unit functional connectivity*

139 Computing the apparent functional connectivity among neurons involved several steps. First, the
140 spikes underlying the calcium fluorescence traces were inferred using a deconvolution algorithm
141 (Friedrich et al., 2017). Next, the data in which the mouse is slow or not moving (below the 10%
142 quantile of the velocity distribution over the track) is removed. The track is then divided into 50
143 spatial bins. The trial-averaged activity in each bin is computed for each cell to create a 'tuning
144 curve' over the belt. The Pearson correlation between the tuning curves of all cell pairs is then
145 computed. To visualize clusters in the cells x cells spatial correlation matrix, the columns/rows
146 were ordered so that highly correlated cells are adjacent. For each neuron, a vector of its
147 correlations with all other cells was generated. In order to determine the similarity between the
148 correlation structures, the pairwise euclidean distances between those vectors were
149 calculated. Using the unweighted pair group method with arithmetic mean (UPGMA), a
150 hierarchical clustering on these measures was conducted (Sokal, 1958). To assess the amount of

151 clustering in the spatial correlation matrices, we computed the average clustering coefficient
152 (Saramäki et al., 2007), a measure which quantifies how many cells with similar firing patterns are
153 similar between each other, averaged over all cells; this coefficient is independent of the ordering
154 of rows/columns.

155

156 **Results**

157 We used 2-photon imaging to record the activity of ensembles of individual neurons (112-732
158 simultaneous cells per session; mean = 380.6, STD = 100.1) in the superficial layers (135 – 160
159 μm ; layer II/III) of RSC in head-fixed mice (Fig. 1.A). Mice were recorded while running on a
160 treadmill belt that had narrow tactile cues laid across the width of the belt in three positions along
161 its length, as well as one auditory cue and one light cue that each activated at specific places in the
162 virtual environment (i.e. belt position). After running for one full lap of the belt, the animals
163 received a 10% sucrose reward. Mice were injected (i.p.) with saline 10 mins prior to task initiation
164 and neural recordings were performed for a 10-minute baseline (“before”) period. They were then
165 injected with either psilocybin (15 mg/kg) or the same volume of saline vehicle 10 mins prior to a
166 second neural recording period. We used both within-session (recording before & after 2nd
167 injection) and within-animal (each received psilocybin or saline on different sessions) controls.
168 Statistical inference of drug effect was determined by 2-way (before/after injection x
169 psilocybin/saline) repeated measures (RM) ANOVA.

170 Psilocybin injection lowered the animals’ movement velocity (Fig. 1.B; RM two-way ANOVA; F
171 (3, 18) = 9.962, $p < 0.001$; Sidak’s post-hoc for psilocybin $p = 0.001$), and reduced the number of
172 trials per minute completed (Fig. 1.C; Mixed-effects model; F (3, 18) = 13.12, $p < 0.0001$; Sidak’s

173 post-hoc $p = 0.002$). Psilocybin did not affect the proportion of time the animals were stationary
174 between the start of a lap and the arrival at the feeder location (stop ratio; Fig. 1.D; RM two-way
175 ANOVA; $F(3, 18) = 5.609$, $p = 0.007$; Sidak's post-hoc for psilocybin $p = 0.636$). The psilocybin-
176 induced retardation of locomotion is consistent with previous reports (Halberstadt et al., 2011;
177 Tylš et al., 2016). The average neural activity rate also decreased after drug administration (Fig.
178 1.E; two-way ANOVA; $F(3, 18) = 7.532$, $p = 0.002$; Sidak's post-hoc $p = 0.045$). A second cohort
179 of animals that only ever received saline showed no significant effect of injection on any of these
180 measures (Supplemental Fig. 1).

181 Many RSC neurons have place-specific activity, activating at specific locations on the belt during
182 each trial (Fig. 2.A), whereas other cells are not selective to particular positions or have high
183 variability. In order to quantify the amount of spatial information conveyed by each neuron, we
184 computed an adjusted form of mutual information (MI) between each cell's activity and belt
185 position (details in methods). This metric captures variance of activity along one lap of the belt, as
186 well as variance from trial to trial (Souza et al., 2018). We then restricted analysis of spatial
187 encoding to the cells that were most selective to position (top quartile of MI distribution).
188 Psilocybin significantly decreased the mean MI of these cells (Fig. 2.B; REML: $F(1, 23) = 6.406$,
189 $p = 0.019$; ROUT ($Q = 1\%$; $n=1$)). We also investigated the average cross correlation of position-
190 dependent cellular activity between trials to assess the stability of spatial tuning. These trial-to-
191 trial correlations decreased after psilocybin but not saline (Fig. 2.C; REML: $F(1, 23) = 19.51$, $p =$
192 0.0002 ; ROUT ($Q = 1\%$; $n=1$)), suggesting less stability of spatial representations after
193 administration of psilocybin as compared to saline.

194 We next sought to determine if psilocybin affected the functional connectivity among cells within
195 the RSC. We computed the pair-wise correlation of activity among all neurons recorded

196 simultaneously during a session, and used hierarchical clustering to order the units so that
197 functionally similar units were adjacent. We applied the same matrix ordering to the activity of the
198 same cells collected after psilocybin administration to visualize any changes in correlation
199 structure (Fig. 2.D). We quantified psychedelic-induced changes in functional connectivity
200 patterns by computing the clustering coefficient of the correlation matrix. This quantifies the
201 statistics of functionally-similar units. It is high when there are multiple clusters, each of which
202 containing functionally-similar units. Psilocybin reduced the clustering coefficient (Fig. 2.E; RM
203 two-way ANOVA; $F(1, 6) = 14.01, p = 0.009$), indicating a loss of functional connectivity
204 structure. In other words, each neuron is activating more independently from the others.

205 We next investigated if these effects of psilocybin on neural activity were mediated by 5-HT_{2A}R
206 by injecting ketanserin (an antagonist of this receptor) prior to the baseline recording period, and
207 then injecting psilocybin prior to the second recording period. We used a randomized schedule of
208 injection after baseline recordings. Treatments were: low dose ketanserin (**k**; 1 mg/kg) followed
209 by low dose psilocybin (**p**; 1.5 mg/kg; $n = 3$); low dose ketanserin followed by high dose psilocybin
210 (**P**; 15 mg/kg; $n = 4$); or high dose ketanserin (**K**; 5 mg/kg) followed by high dose psilocybin ($n =$
211 3). Low dose ketanserin blocked the effects of high or low dose psilocybin on behaviour, firing
212 rate, MI, trial-to-trial correlation, and clustering of cross-correlations (Fig. 3. C-D; Supplemental
213 Fig. 2; Supplemental Table 1). The high dose ketanserin did not fully block the effects of high
214 psilocybin on MI (Fig. 3.A; RM two-way ANOVA; $F(3, 6) = 13.53, p = 0.004$; Sidak's post-hoc
215 $p = 0.046$) or firing rate (Fig. 3.B; RM two-way ANOVA; $F(3, 6) = 10.40, p = 0.009$; Sidak's
216 post-hoc $p = 0.013$). Nonetheless, it appears that ketanserin blocks or reduces the effects of
217 psilocybin on both behaviour and neural activity, suggesting that 5-HT_{2A}R are involved in the
218 phenomena.

219 **Discussion**

220 In this study, psilocybin reduced locomotion, decreased spatial information encoded by RSC cells,
221 and decreased functional connectivity among RSC neurons. The 5-HT_{2A} antagonist ketanserin
222 blocked the behavioural effects and prevented the loss of spatial information at a dose of 1 mg/kg.
223 Unexpectedly, the higher dose of ketanserin (5 mg/kg) did not fully block effects of psilocybin on
224 firing rate and MI. Nonetheless, the preponderance of evidence suggests that the effects of
225 psilocybin in this study are primarily mediated by 5-HT_{2A}R.

226 The administration of psilocybin reduced locomotion speed in the present data, similar to previous
227 reports (Halberstadt et al., 2011; Tylš et al., 2016). Psilocybin also decreased the mean activity
228 rate of RSC neurons in this study, which contrasts the increase in RSC activity rate by the non-
229 classic psychedelic ibogaine in our previous study using the same experimental apparatus (Ivan et
230 al., 2023). We are unaware of other prior studies examining effects of psychedelics on RSC neuron
231 activity, but there are some limited data in functionally related brain structures. Lower doses of
232 psilocybin (2 mg/kg) increased the firing rate of ACC neurons in head-fixed mice running on a
233 treadmill (Golden and Chadderton, 2022). Similarly, 5-MeO-DMT also increased activity rates in
234 a majority of neurons recorded in layer V of ACC in anesthetized rats (Riga et al., 2014). This
235 psychedelic and psilocybin increase excitatory post-synaptic currents of pyramidal neurons in
236 brain slices of prefrontal cortex (Shao et al., 2021; Vargas et al., 2023). In contrast, a psilocybin-
237 containing extract decreased neuronal spiking in the majority of CA1 pyramidal neurons in brain-
238 slices of HPC (Moldavan et al., 2000). It is unclear if these discrepant effects of psychedelics on
239 firing rate is due to dose, brain structure, locomotion, or other factors.

240 Psilocybin caused a large-scale reorganization of the relationship of activity among RSC neurons.
241 After psilocybin administration, the dominant motifs of pair-wise correlation structure are

242 dispersed, indicating that the most common patterns of RSC activity during baseline largely
243 vanish. This pattern is consistent across sessions and animals, indicating that acute psilocybin
244 causes a restructuring of functional connectivity (FC) among neurons. This effect can be partially
245 explained by the destabilization of positional signaling. In human fMRI studies, psychedelic drugs
246 have been generally reported to increase the distribution of activity covariance motifs among brain
247 regions (Tagliazucchi et al., 2014; Atasoy et al., 2017), and promote cortical desynchronization
248 (Muthukumaraswamy et al., 2013; Riga et al., 2018). Psilocybin has been shown to particularly
249 affect the FC within the default-mode network (DMN), which includes RSC (Carhart-Harris et al.,
250 2012; Roseman et al., 2014; Daws et al., 2022). This effect of psilocybin to reduce FC in the DMN
251 has also been reported in fMRI studies of rodents (Grandjean et al., 2021). The psychedelic-
252 associated loss of functional connectivity is often associated with ego-dissolution, which was
253 shown to correlate with decreased FC between the parahippocampal and retrosplenial cortex
254 (Carhart-Harris et al., 2016; Lebedev et al., 2016). Both psilocybin and LSD significantly increase
255 the ‘complexity’ of functional connectivity networks in the neocortex (Varley et al., 2020; Girm et
256 al., 2022). Our results are consistent with these reports, and demonstrate similar dynamical changes
257 at the cellular level within the RSC.

258 Acute psilocybin administration decreased the stability of RSC neuron encoding of position,
259 shown by the reduced mutual information and trial-to-trial correlation of individual neurons. Many
260 RSC cells encoded specific locations on the belt before psychedelic administration, as shown
261 previously (Mao et al., 2017), but these cells are destabilized by psilocybin, similar to the effect
262 of the non-classic psychedelic ibogaine (Ivan et al., 2023). However, despite the high dosage of
263 psilocybin used here, the changes in spatial encoding were surprisingly weak as compared to those
264 evoked by a moderate dose of ibogaine (Ivan et al., 2023). Multiple regions in the neocortex encode

265 position, environmental cues, and spatial information (Mashhoori et al., 2018; Esteves et al., 2021),
266 which can provide a framework for navigation and context-dependent learning (Gruber and
267 McDonald, 2012; Chang et al., 2020). Reports of human perceptual experience is consistent with
268 psychedelic-based disruption of this information. Psychedelics often disrupt the sense of space and
269 time, causing disorientation and a feeling of spacelessness (Carbonaro et al., 2016; Garcia-Romeu
270 et al., 2016; Smigielski et al., 2019). It is unclear if the altered encoding of space in RSC is more
271 due to the direct action of psilocybin in RSC, or to alterations of afferent information. RSC
272 positional information relies on hippocampal processing (Esteves et al., 2021) in order to form and
273 maintain the cognitive map (McNaughton et al., 2006). Psilocybin not only affects 5-HT receptors,
274 but also alters glutamate levels in both the mPFC and the HPC (Mason et al., 2020). Interestingly,
275 higher glutamate in mPFC correlated with negative experiences, whereas lower glutamate in HPC
276 was associated with a pleasant state of ego dissolution. Rodent studies have likewise found that
277 psilocybin or its active form psilocin can affect dopamine, serotonin, glutamate, and GABA levels
278 in the frontal cortex and/or striatum (Sakashita et al., 2015; Wojtas et al., 2022). These data suggest
279 that the effect of psilocybin on RSC activity could involve modulation of several neurotransmitter
280 systems in RSC and afferent structures.

281 Despite affecting several neurotransmitter systems, psilocybin exerts its psychoactive effects
282 primarily through the 5-HT_{2A} receptor. The occupancy of these receptors in the neocortex relates
283 closely to the intensity of the psychedelic effect (Madsen et al., 2019; Kringelbach et al., 2020).
284 We found that blocking these receptors with ketanserin reduced the majority of the behavioural
285 and neural activity effects caused by psilocybin. Interestingly, the low dose fully blocked effects,
286 whereas the high dose did not. Prior rodent work has similarly shown only partial blockade of
287 psilocybin effects at behavioural and synaptic levels with ketanserin or closely related molecules

288 (Moldavan et al., 2000; Hesselgrave et al., 2021; Torrado Pacheco et al., 2023). Indeed, other 5-
289 HT receptors are involved in modulating behaviour. For instance, 5-HT_{1A} and 5-HT_{2C} receptors
290 also contribute significantly the suppressing effect of psilocin on locomotion and investigatory
291 behaviour in rats (Tylš et al., 2016) and mice (Halberstadt et al., 2011). Moreover, the effects of
292 5-HT blockade depend on cellular physiology and/or phenotype. For instance, systemic
293 administration of ketanserin reduced conditioned freezing in rats bred to display enhanced
294 freezing, but exerted the opposite effect in low-freezing animals (León et al., 2017). Besides the
295 possible involvement of multiple 5-HT receptor subtypes, it is also possible that the
296 pharmacodynamics contributed to the inability of ketanserin to fully block effects of psilocybin on
297 spatial encoding in the present data, as psilocybin was administered 30 min after the antagonist. In
298 previous reports, ketanserin pretreatment only partially reduced psilocybin-induced head-twitch
299 behaviour when administered 1h before the psychedelic (Hesselgrave et al., 2021), but abolished
300 it when administered 10 minutes before psilocybin (Shao et al., 2021). In sum, our data are
301 consistent with prior studies in that they suggest some involvement of 5-HT_{2A} receptors in the
302 effects of psilocybin, but do not rule out contributions of other neurotransmitter systems.

303 **Conclusion**

304 Although several fMRI studies in humans and rodents have indicated that psychedelics alter
305 mesoscale brain activity levels and cross-regional coordination, little is known about how these
306 drugs affect information representation and processing at the cellular level. The present data
307 suggest that activity of individual RSC neurons become discoordinated from one another, and
308 overall activity rates are reduced. These data are consistent with mesoscale effects reported in
309 fMRI studies. Despite the discoordination among neurons, the representation of spatial position by
310 individual neurons was only mildly impaired. This was surprising because of the high dose of

311 psilocybin administered (15 mg/kg), which in humans would evoke profound changes in
312 mentation. We therefore speculate that either the drug's effect on mentation is less intense in these
313 mice than is typical in humans, or that psychedelics effects are manifested by subtle changes to
314 neural encoding that are difficult to identify in the present experimental design.

315

316 **Acknowledgments**

317 We would like to thank Adam Neumann for technical support and Dr. HaoRan Chang for helpful
318 discussions. Funding provided by: Natural Sciences and Engineering Council of Canada, New
319 Frontiers Research Fund, Alberta Innovates, Beswick Fellowship, Canadian Institute of Health
320 Research.

321 Author Contributions: V.E.I. and A.J.G. designed research, V.E.I. and I.M.E. performed research,
322 M.M. contributed tools, V.E.I., D.P.T-C, and I.M.E. analyzed data, V.E.I., D.P.T-C, A.L., B.L.M.,
323 and A.J.G. wrote the paper.

324 Competing Interest Statement: The authors declare no competing interests.

325

326

327

328

329

330

331 **References**

- 332 Alexander, A.S., and Nitz, D.A. (2015). Retrosplenial cortex maps the conjunction of internal and external
333 spaces. *Nature Neuroscience* 18(8), 1143-1151. doi: 10.1038/nn.4058.
- 334 Andrade, R. (2011). Serotonergic regulation of neuronal excitability in the prefrontal cortex.
335 *Neuropharmacology* 61(3), 382-386. doi: <https://doi.org/10.1016/j.neuropharm.2011.01.015>.
- 336 Atasoy, S., Roseman, L., Kaelen, M., Kringelbach, M.L., Deco, G., and Carhart-Harris, R.L. (2017).
337 Connectome-harmonic decomposition of human brain activity reveals dynamical repertoire re-
338 organization under LSD. *Scientific Reports* 7(1), 17661. doi: 10.1038/s41598-017-17546-0.
- 339 Carbonaro, T.M., Bradstreet, M.P., Barrett, F.S., MacLean, K.A., Jesse, R., Johnson, M.W., et al. (2016).
340 Survey study of challenging experiences after ingesting psilocybin mushrooms: Acute and
341 enduring positive and negative consequences. *Journal of Psychopharmacology* 30(12), 1268-
342 1278. doi: 10.1177/0269881116662634.
- 343 Carhart-Harris, R.L., Erritzoe, D., Williams, T., Stone, J.M., Reed, L.J., Colasanti, A., et al. (2012). Neural
344 correlates of the psychedelic state as determined by fMRI studies with psilocybin. *Proceedings*
345 *of the National Academy of Sciences* 109(6), 2138-2143. doi: 10.1073/pnas.1119598109.
- 346 Carhart-Harris, R.L., Muthukumaraswamy, S., Roseman, L., Kaelen, M., Droog, W., Murphy, K., et al.
347 (2016). Neural correlates of the LSD experience revealed by multimodal neuroimaging.
348 *Proceedings of the National Academy of Sciences* 113(17), 4853-4858. doi:
349 10.1073/pnas.1518377113.
- 350 Carhart-Harris, R.L., Roseman, L., Bolstridge, M., Demetriou, L., Pannekoek, J.N., Wall, M.B., et al.
351 (2017b). Psilocybin for treatment-resistant depression: fMRI-measured brain mechanisms.
352 *Scientific reports* 7(1), 1-11.
- 353 Carter, O.L., Burr, D.C., Pettigrew, J.D., Wallis, G.M., Hasler, F., and Vollenweider, F.X. (2005). Using
354 psilocybin to investigate the relationship between attention, working memory, and the
355 serotonin 1A and 2A receptors. *Journal of Cognitive neuroscience* 17(10), 1497-1508.
- 356 Chang, H., Esteves, I.M., Neumann, A.R., Sun, J., Mohajerani, M.H., and McNaughton, B.L. (2020).
357 Coordinated activities of retrosplenial ensembles during resting-state encode spatial landmarks.
358 *Philosophical Transactions of the Royal Society B: Biological Sciences* 375(1799), 20190228. doi:
359 doi:10.1098/rstb.2019.0228.
- 360 Daws, R.E., Timmermann, C., Giribaldi, B., Sexton, J.D., Wall, M.B., Erritzoe, D., et al. (2022). Increased
361 global integration in the brain after psilocybin therapy for depression. *Nature Medicine* 28(4),
362 844-851. doi: 10.1038/s41591-022-01744-z.
- 363 Esteves, I.M., Chang, H., Neumann, A.R., Sun, J., Mohajerani, M.H., and McNaughton, B.L. (2021). Spatial
364 Information Encoding across Multiple Neocortical Regions Depends on an Intact Hippocampus.
365 *The Journal of Neuroscience* 41(2), 307. doi: 10.1523/JNEUROSCI.1788-20.2020.
- 366 Fisk, G.D., and Wyss, J.M. (1999). Associational projections of the anterior midline cortex in the rat:
367 intracingulate and retrosplenial connections. *Brain Research* 825(1), 1-13. doi:
368 [https://doi.org/10.1016/S0006-8993\(99\)01182-8](https://doi.org/10.1016/S0006-8993(99)01182-8).
- 369 Friedrich, J., Zhou, P., and Paninski, L. (2017). Fast online deconvolution of calcium imaging data. *PLOS*
370 *Computational Biology* 13(3), e1005423. doi: 10.1371/journal.pcbi.1005423.
- 371 Garcia-Romeu, A., Kersgaard, B., and Addy, P.H. (2016). Clinical applications of hallucinogens: A review.
372 *Experimental and clinical psychopharmacology* 24(4), 229-268. doi: 10.1037/pha0000084.
- 373 Girn, M., Roseman, L., Bernhardt, B., Smallwood, J., Carhart-Harris, R., and Nathan Spreng, R. (2022).
374 Serotonergic psychedelic drugs LSD and psilocybin reduce the hierarchical differentiation of
375 unimodal and transmodal cortex. *NeuroImage* 256, 119220. doi:
376 <https://doi.org/10.1016/j.neuroimage.2022.119220>.

377 Golden, C.T., and Chadderton, P. (2022). Psilocybin reduces low frequency oscillatory power and
378 neuronal phase-locking in the anterior cingulate cortex of awake rodents. *Scientific Reports*
379 12(1), 12702. doi: 10.1038/s41598-022-16325-w.

380 Grandjean, J., Buehlmann, D., Buerge, M., Sigrist, H., Seifritz, E., Vollenweider, F.X., et al. (2021).
381 Psilocybin exerts distinct effects on resting state networks associated with serotonin and
382 dopamine in mice. *NeuroImage* 225, 117456. doi:
383 <https://doi.org/10.1016/j.neuroimage.2020.117456>.

384 Gruber, A.J., and McDonald, R.J. (2012). Context, emotion, and the strategic pursuit of goals:
385 interactions among multiple brain systems controlling motivated behavior. *Front Behav Neurosci*
386 6(50), 50. doi: 10.3389/fnbeh.2012.00050.

387 Halberstadt, A.L., Koedood, L., Powell, S.B., and Geyer, M.A. (2011). Differential contributions of
388 serotonin receptors to the behavioral effects of indoleamine hallucinogens in mice. *Journal of*
389 *psychopharmacology* 25(11), 1548-1561.

390 Hesselgrave, N., Troppoli, T.A., Wulff, A.B., Cole, A.B., and Thompson, S.M. (2021). Harnessing
391 psilocybin: antidepressant-like behavioral and synaptic actions of psilocybin are independent of
392 5-HT2R activation in mice. *Proceedings of the National Academy of Sciences* 118(17),
393 e2022489118. doi: 10.1073/pnas.2022489118.

394 Iaria, G., Chen, J.-K., Guariglia, C., Ptito, A., and Petrides, M. (2007). Retrosplenial and hippocampal brain
395 regions in human navigation: complementary functional contributions to the formation and use
396 of cognitive maps. *European Journal of Neuroscience* 25(3), 890-899. doi:
397 <https://doi.org/10.1111/j.1460-9568.2007.05371.x>.

398 Ivan, V.E., Tomàs-Cuesta, D.P., Esteves, I.M., Curic, D., Mohajerani, M., McNaughton, B.L., et al. (2023).
399 The non-classic psychedelic ibogaine disrupts cognitive maps. *Biological Psychiatry Global Open*
400 *Science*. doi: <https://doi.org/10.1016/j.bpsgos.2023.07.008>.

401 Keene, C.S., and Bucci, D.J. (2009). Damage to the retrosplenial cortex produces specific impairments in
402 spatial working memory. *Neurobiology of Learning and Memory* 91(4), 408-414. doi:
403 <https://doi.org/10.1016/j.nlm.2008.10.009>.

404 Komater, M., Schmidt, A., Bachmann, R., Studerus, E., Seifritz, E., and Vollenweider, F.X. (2012).
405 Psilocybin Biases Facial Recognition, Goal-Directed Behavior, and Mood State Toward Positive
406 Relative to Negative Emotions Through Different Serotonergic Subreceptors. *Biological*
407 *Psychiatry* 72(11), 898-906. doi: <https://doi.org/10.1016/j.biopsych.2012.04.005>.

408 Kringelbach, M.L., Cruzat, J., Cabral, J., Knudsen, G.M., Carhart-Harris, R., Whybrow, P.C., et al. (2020).
409 Dynamic coupling of whole-brain neuronal and neurotransmitter systems. *Proceedings of the*
410 *National Academy of Sciences* 117(17), 9566-9576. doi: 10.1073/pnas.1921475117.

411 Lebedev, A.V., Kaelen, M., Lövdén, M., Nilsson, J., Feilding, A., Nutt, D.J., et al. (2016). LSD-induced
412 entropic brain activity predicts subsequent personality change. *Human Brain Mapping* 37(9),
413 3203-3213. doi: <https://doi.org/10.1002/hbm.23234>.

414 León, L.A., Castro-Gomes, V., Zárate-Guerrero, S., Corredor, K., Mello Cruz, A.P., Brandão, M.L., et al.
415 (2017). Behavioral Effects of Systemic, Infralimbic and Prelimbic Injections of a Serotonin 5-HT2A
416 Antagonist in Carioca High- and Low-Conditioned Freezing Rats. *Frontiers in Behavioral*
417 *Neuroscience* 11. doi: 10.3389/fnbeh.2017.00117.

418 Madsen, M.K., Fisher, P.M., Burmester, D., Dyssegaard, A., Stenbæk, D.S., Kristiansen, S., et al. (2019).
419 Psychedelic effects of psilocybin correlate with serotonin 2A receptor occupancy and plasma
420 psilocin levels. *Neuropsychopharmacology* 44(7), 1328-1334. doi: 10.1038/s41386-019-0324-9.

421 Mao, D., Kandler, S., McNaughton, B.L., and Bonin, V. (2017). Sparse orthogonal population
422 representation of spatial context in the retrosplenial cortex. *Nature Communications* 8(1), 243.
423 doi: 10.1038/s41467-017-00180-9.

424 Mao, D., Neumann, A.R., Sun, J., Bonin, V., Mohajerani, M.H., and McNaughton, B.L. (2018).
425 Hippocampus-dependent emergence of spatial sequence coding in retrosplenial cortex.
426 *Proceedings of the National Academy of Sciences* 115(31), 8015. doi: 10.1073/pnas.1803224115.

427 Mashhoori, A., Hashemnia, S., McNaughton, B.L., Euston, D.R., and Gruber, A.J. (2018). Rat anterior
428 cingulate cortex recalls features of remote reward locations after disfavoured reinforcements.
429 *eLife* 7, e29793. doi: 10.7554/eLife.29793.

430 Mason, N.L., Kuypers, K.P.C., Müller, F., Reckweg, J., Tse, D.H.Y., Toennes, S.W., et al. (2020). Me, myself,
431 bye: regional alterations in glutamate and the experience of ego dissolution with psilocybin.
432 *Neuropsychopharmacology* 45(12), 2003-2011. doi: 10.1038/s41386-020-0718-8.

433 McNaughton, B.L., Battaglia, F.P., Jensen, O., Moser, E.I., and Moser, M.-B. (2006). Path integration and
434 the neural basis of the 'cognitive map'. *Nature Reviews Neuroscience* 7(8), 663-678. doi:
435 10.1038/nrn1932.

436 Michaiel, A.M., Parker, P.R.L., and Niell, C.M. (2019). A Hallucinogenic Serotonin-2A Receptor Agonist
437 Reduces Visual Response Gain and Alters Temporal Dynamics in Mouse V1. *Cell Reports* 26(13),
438 3475-3483. e3474. doi: <https://doi.org/10.1016/j.celrep.2019.02.104>.

439 Moldavan, M., Solomko, E.F., Grodzinskaya, A.A., Storozhuk, V.M., and Lomborg, M.L. (2000).
440 Neurotropic Effect of Extracts from the Hallucinogenic Mushroom *Psilocybe cubensis* (Earle)
441 Sing.(Agaricomycetidae). In Vitro Studies. *International Journal of Medicinal Mushrooms* 2(4).

442 Muthukumaraswamy, S.D., Carhart-Harris, R.L., Moran, R.J., Brookes, M.J., Williams, T.M., Erntizoe, D., et
443 al. (2013). Broadband Cortical Desynchronization Underlies the Human Psychedelic State. *The*
444 *Journal of Neuroscience* 33(38), 15171-15183. doi: 10.1523/jneurosci.2063-13.2013.

445 O'Keefe, J., and Nadel, L. (1978). *The Hippocampus as a Cognitive Map*. Oxford: Clarendon Press.

446 Pachitariu, M., Stringer, C., Dipoppa, M., Schröder, S., Rossi, L.F., Dagleish, H., et al. (2017). Suite2p:
447 beyond 10,000 neurons with standard two-photon microscopy. *Biorxiv*.

448 Pnevmatikakis, Eftychios A., Soudry, D., Gao, Y., Machado, T.A., Merel, J., Pfau, D., et al. (2016).
449 Simultaneous Denoising, Deconvolution, and Demixing of Calcium Imaging Data. *Neuron* 89(2),
450 285-299. doi: <https://doi.org/10.1016/j.neuron.2015.11.037>.

451 Quednow, B.B., Komater, M., Geyer, M.A., and Vollenweider, F.X. (2012). Psilocybin-Induced Deficits in
452 Automatic and Controlled Inhibition are Attenuated by Ketanserin in Healthy Human Volunteers.
453 *Neuropsychopharmacology* 37(3), 630-640. doi: 10.1038/npp.2011.228.

454 Riga, M.S., Lladó-Pelfort, L., Artigas, F., and Celada, P. (2018). The serotonin hallucinogen 5-MeO-DMT
455 alters cortico-thalamic activity in freely moving mice: Regionally-selective involvement of 5-
456 HT1A and 5-HT2A receptors. *Neuropharmacology* 142, 219-230. doi:
457 <https://doi.org/10.1016/j.neuropharm.2017.11.049>.

458 Riga, M.S., Soria, G., Tudela, R., Artigas, F., and Celada, P. (2014). The natural hallucinogen 5-MeO-DMT,
459 component of Ayahuasca, disrupts cortical function in rats: reversal by antipsychotic drugs.
460 *International Journal of Neuropsychopharmacology* 17(8), 1269-1282. doi:
461 10.1017/S1461145714000261.

462 Roseman, L., Leech, R., Feilding, A., Nutt, D.J., and Carhart-Harris, R.L. (2014). The effects of psilocybin
463 and MDMA on between-network resting state functional connectivity in healthy volunteers.
464 *Frontiers in Human Neuroscience* 8. doi: 10.3389/fnhum.2014.00204.

465 Sakashita, Y., Abe, K., Katagiri, N., Kambe, T., Saitoh, T., Utsunomiya, I., et al. (2015). Effect of psilocin on
466 extracellular dopamine and serotonin levels in the mesoaccumbens and mesocortical pathway
467 in awake rats. *Biological and Pharmaceutical Bulletin* 38(1), 134-138.

468 Saramäki, J., Kivelä, M., Onnela, J.-P., Kaski, K., and Kertész, J. (2007). Generalizations of the clustering
469 coefficient to weighted complex networks. *Physical Review E* 75(2), 027105. doi:
470 10.1103/PhysRevE.75.027105.

471 Shao, L.-X., Liao, C., Gregg, I., Davoudian, P.A., Savalia, N.K., Delagarza, K., et al. (2021). Psilocybin
472 induces rapid and persistent growth of dendritic spines in frontal cortex in vivo. *Neuron* 109(16),
473 2535-2544.e2534. doi: <https://doi.org/10.1016/j.neuron.2021.06.008>.

474 Shibata, H., Kondo, S., and Naito, J. (2004). Organization of retrosplenial cortical projections to the
475 anterior cingulate, motor, and prefrontal cortices in the rat. *Neuroscience Research* 49(1), 1-11.
476 doi: <https://doi.org/10.1016/j.neures.2004.01.005>.

477 Smigielski, L., Kometer, M., Scheidegger, M., Krähenmann, R., Huber, T., and Vollenweider, F.X. (2019).
478 Characterization and prediction of acute and sustained response to psychedelic psilocybin in a
479 mindfulness group retreat. *Scientific Reports* 9(1), 14914. doi: 10.1038/s41598-019-50612-3.

480 Sokal, R.R. (1958). A statistical method for evaluating systematic relationships. *Univ. Kansas, Sci. Bull.* 38,
481 1409-1438.

482 Souza, B.C., Pavão, R., Belchior, H., and Tort, A.B.L. (2018). On Information Metrics for Spatial Coding.
483 *Neuroscience* 375, 62-73. doi: <https://doi.org/10.1016/j.neuroscience.2018.01.066>.

484 Spain, A., Howarth, C., Khrapitchev, A.A., Sharp, T., Sibson, N.R., and Martin, C. (2015). Neurovascular
485 and neuroimaging effects of the hallucinogenic serotonin receptor agonist psilocin in the rat
486 brain. *Neuropharmacology* 99, 210-220. doi:
487 <https://doi.org/10.1016/j.neuropharm.2015.07.018>.

488 Tagliazucchi, E., Carhart-Harris, R., Leech, R., Nutt, D., and Chialvo, D.R. (2014). Enhanced repertoire of
489 brain dynamical states during the psychedelic experience. *Human Brain Mapping* 35(11), 5442-
490 5456. doi: 10.1002/hbm.22562.

491 Torrado Pacheco, A., Olson, R.J., Garza, G., and Moghaddam, B. (2023). Acute psilocybin enhances
492 cognitive flexibility in rats. *Neuropsychopharmacology : official publication of the American*
493 *College of Neuropsychopharmacology*. doi: 10.1038/s41386-023-01545-z.

494 Tylš, F., Páleníček, T., Kadeřábek, L., Lipski, M., Kubešová, A., and Horáček, J. (2016). Sex differences and
495 serotonergic mechanisms in the behavioural effects of psilocin. *Behavioural Pharmacology*
496 27(4), 309-320.

497 Vargas, M.V., Dunlap, L.E., Dong, C., Carter, S.J., Tombari, R.J., Jami, S.A., et al. (2023). Psychedelics
498 promote neuroplasticity through the activation of intracellular 5-HT2A receptors. *Science*
499 379(6633), 700-706. doi: doi:10.1126/science.adf0435.

500 Varley, T.F., Carhart-Harris, R., Roseman, L., Menon, D.K., and Stamatakis, E.A. (2020). Serotonergic
501 psychedelics LSD & psilocybin increase the fractal dimension of cortical brain activity in spatial
502 and temporal domains. *NeuroImage* 220, 117049. doi:
503 <https://doi.org/10.1016/j.neuroimage.2020.117049>.

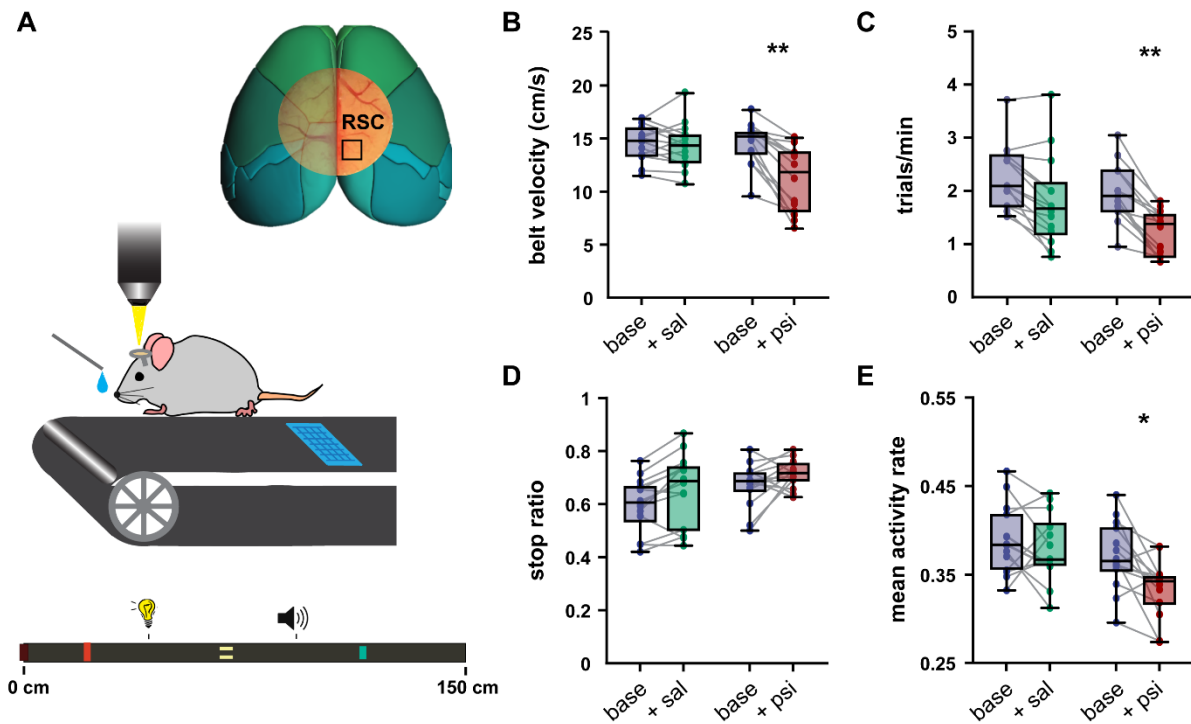
504 Vinh, N.X., Epps, J., and Bailey, J. (2010). Information theoretic measures for clusterings comparison:
505 Variants, properties, normalization and correction for chance. *The Journal of Machine Learning*
506 *Research* 11, 2837-2854.

507 Vollenweider, F.X., Vollenweider-Scherpenhuyzen, M.F.I., Bäbler, A., Vogel, H., and Hell, D. (1998).
508 Psilocybin induces schizophrenia-like psychosis in humans via a serotonin-2 agonist action.
509 *NeuroReport* 9(17).

510 Wojtas, A., Bysiek, A., Wawrzczak-Bargiela, A., Szych, Z., Majcher-Maślanka, I., Herian, M., et al. 2022.
511 Effect of Psilocybin and Ketamine on Brain Neurotransmitters, Glutamate Receptors, DNA and
512 Rat Behavior. *International Journal of Molecular Sciences* [Online], 23(12).

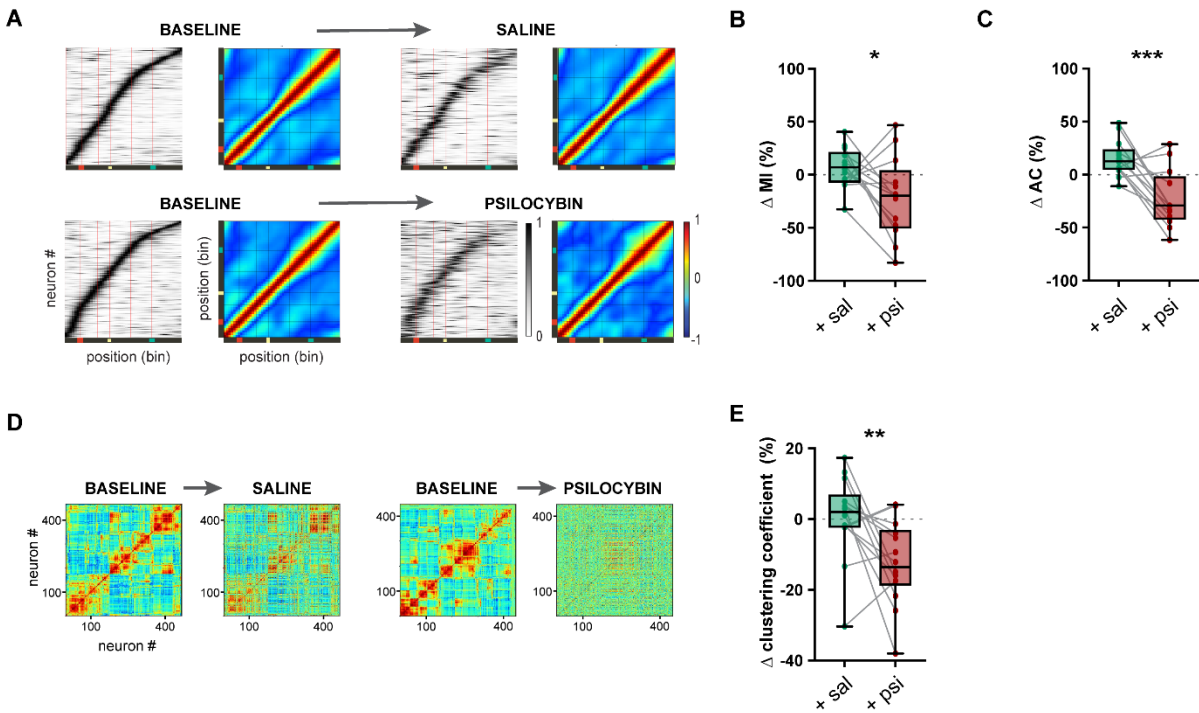
513 Wyass, J.M., and Van Groen, T. (1992). Connections between the retrosplenial cortex and the
514 hippocampal formation in the rat: A review. *Hippocampus* 2(1), 1-11. doi:
515 10.1002/hipo.450020102.

516



517

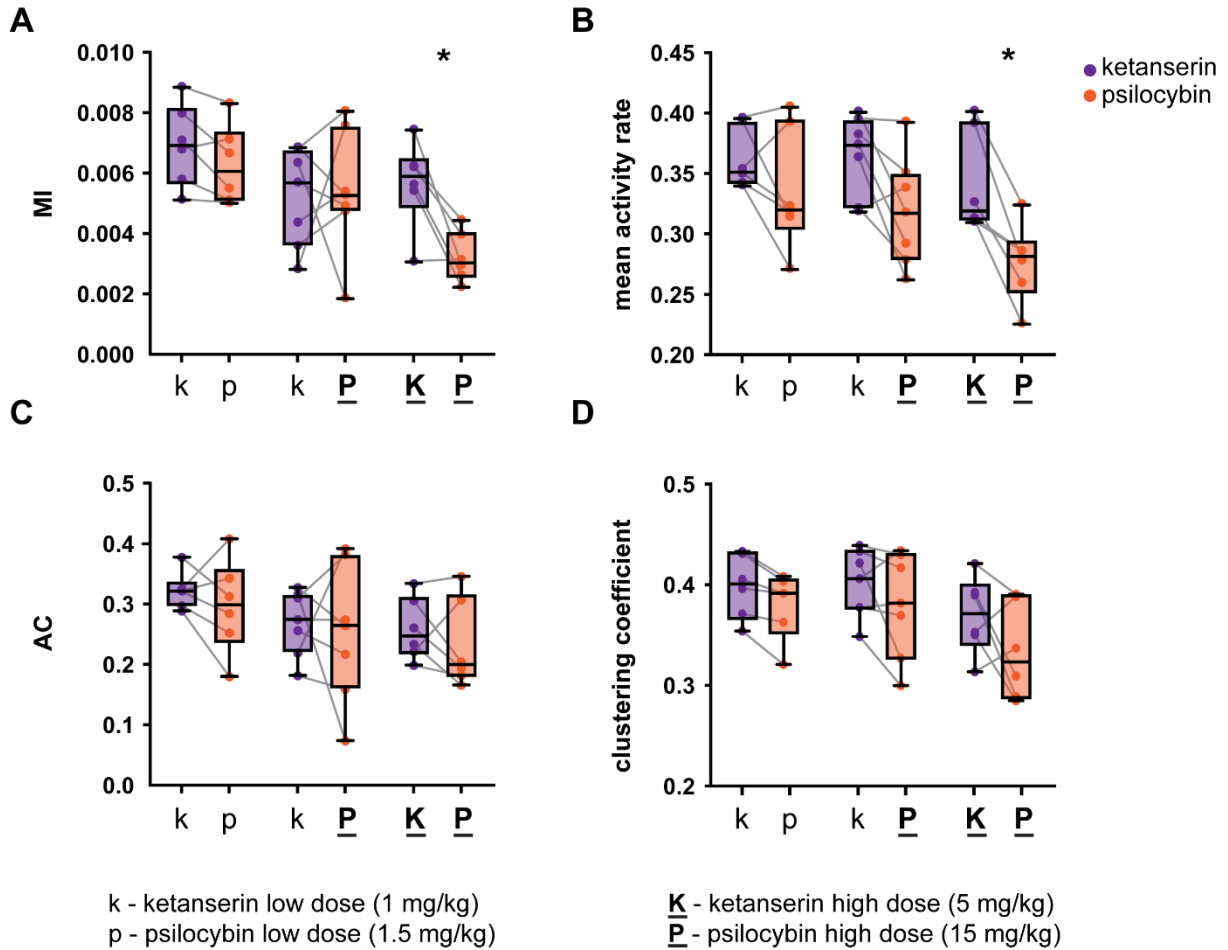
518 **Fig. 1. Behavioural effects of psilocybin.** A. Illustration of experimental setup and location of the
 519 field of view over RSC (inset). Symbols on the treadmill belt indicate approximate locations of
 520 tactile cues, as well as locations of visual and auditory cues. B. Box plots of the belt velocity
 521 before/after saline/psilocybin administration. C. Number of trials per minute. D. Proportion of time
 522 that mice were stationary during a trial. E. Mean activity rate of all neurons recorded simultaneously
 523 in a session. Statistical significance ($p < 0.05$) is indicated by ‘*’, and ($p < 0.01$) is indicated by ‘**’.
 524 Dots are averages from each session.



525
 526 **Fig. 2. Effects of psilocybin on spatial encoding by neurons in the RSC.** A. Leftward panels
 527 (black/white) show session-averaged activity of all position-tuned cells ordered by lag to peak
 528 activity. The abscissa is treadmill belt position, the ordinate is individual neurons, and shade
 529 indicates average normalized activity density of each neuron along the belt. Darker shade is higher
 530 activity. Rightward panels (color) shows the mean autocorrelation of activity for the same cells.
 531 Grouped panels show aggregated data from the same sessions before (left two panels) and after
 532 (right two panels) injection. Sessions testing saline (top) were separate from those testing
 533 psilocybin (bottom). The cue zones are indicated by red vertical lines. B. Box plots and individual
 534 session-averaged values of percentage change of the mean mutual information (MI) with respect
 535 to baseline within each recording session. C. Percentage change of the average trial-to-trial
 536 correlation (AC) with respect to baseline within each recording day. D. Pairwise correlation
 537 matrices of unit activity in one representative session before/after saline (top row) and before/after
 538 psilocybin (bottom row). E. Percentage change of the means connectivity coefficients within each

539 recording session. Statistical significance ($p < 0.05$) is indicated by ‘*’, ($p < 0.01$) is indicated by
 540 ‘**’, and ($p < 0.001$) is indicated by ‘***’.

541



542

543 **Fig. 3. Effects of ketanserin pretreatment on psilocybin-mediated changes in RSC spatial**

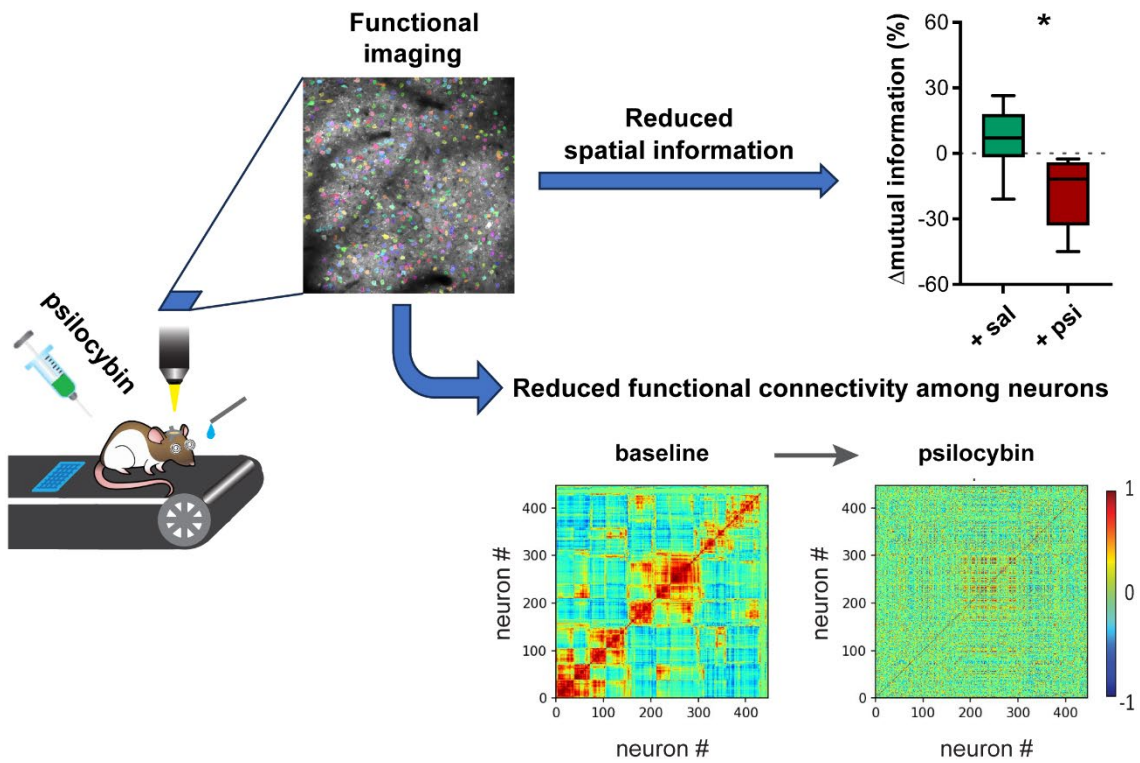
544 **encoding.** A. Box plots and individual values of adjusted mutual information (MI) for the different

545 dose combinations with either low (k; 1 mg/kg) or high (k; 5 mg/kg) ketanserin pretreatment and

546 low (p; 1.5 mg/kg) or high (P; 15 mg/kg) psilocybin administration. B. Box plots and individual

547 values of average firing rates for each group. C. Mean trial-to-trial correlations (AC). D. Mean

548 connectivity coefficients. Statistical significance ($p < 0.05$) is indicated by ‘*’.



549

550

551 **Graphical abstract.** Administration of psilocybin in head-fixed mice navigating on a treadmill
 552 decreases the place specificity and functional connectivity among simultaneously recorded
 553 neurons in the retrosplenial cortex.